Available online at www.sciencedirect.com
ScienceDirect
Journal of Molecular Spectroscopy 243 (2007) 62–68
Journal of MOLECULAR SPECTROSCOPY
www.elsevier.com/locate/jms

Fourier transform spectroscopy of new emission systems of NbN in the visible region

R.S. Ram [a,*], P.F. Bernath [a,b,c]

[a] Department of Chemistry, University of Arizona, Tucson, AZ 85721, USA
[b] Department of Chemistry, University of Waterloo, Waterloo, Ont., Canada N2L 3G1
[c] Department of Chemistry, University of York, Heslington, York YO10 5DD, UK

Received 22 January 2007; in revised form 20 March 2007
Available online 7 April 2007

Abstract

The emission spectrum of NbN has been reinvestigated in the 8000–35000 cm^{-1} region using a Fourier transform spectrometer and two groups of new bands were observed. The bands observed in the 18000–20000 cm^{-1} region have been assigned to a new $^3\Pi$–$X^3\Delta$ transition. Three bands with R heads near 19463.8, 19659.0 and 19757.0 cm^{-1} have been assigned as 0–0 bands of the $^3\Pi_2$–$X^3\Delta_3$, $^3\Pi_1$–$X^3\Delta_2$ and $^3\Pi_{0\pm}$–$X^3\Delta_1$ subbands, respectively, of this new transition. Three additional $\Delta\Omega = 0$ bands have been observed in the 24000–26000 cm^{-1} region. A 0–0 band with an R head near 25409.9 cm^{-1} has been assigned as a $\Delta\Omega = 0$ transition having $X^3\Delta_2$ as its lower state while two additional bands with heads near 25518.7 and 25534.8 cm^{-1} were found to be $\Delta\Omega = 0$ bands having $X^3\Delta_1$ as the common lower state. Two of these three bands are perhaps subbands of a $^3\Delta$–$X^3\Delta$ transition. Most of the excited levels are affected by perturbations.

Keywords: Fourier transform spectroscopy; Transition metal nitrides

1. Introduction

Diatomic transition metal nitrides provide simple models for the study of metal–nitrogen bonding in inorganic chemistry. The interaction of transition metals with nitrogen has important application in catalysis, surface science and ab initio calculations. Transition metal atoms have relatively high abundances in many stars [1–3] and several transition metal hydrides and oxides have also been detected. There is strong possibility that transition metal nitrides may also be found. So far nitride molecules have not been observed in stellar atmospheres, in part due to lack of precise spectroscopic data required for a meaningful search in the complex stellar spectra. In recent years, the electronic spectra of several transition metal nitrides have been analyzed at high resolution [4–15] and considerable progress has been made in theoretical studies [15–24]. In some cases the ab initio calculations have greatly added in the analysis of the complex spectra.

NbN has been studied extensively using various experimental techniques and some high quality ab initio calculations are also available. Almost all of the observed low-lying electronic states of NbN have been found to be consistent with ab initio predictions. The electronic spectra of NbN were first observed by Dunn and Rao in 1969 [25]. They observed a $^3\Phi$–$^3\Delta$ transition in the visible region and initially named it as $A^3\Phi$–$X^3\Delta$. This transition was later investigated by Féménias et al. [26] and more recently by Azuma et al. [27,28], and molecular constants including hyperfine parameters have been determined. This transition was renamed as $B^3\Phi$–$X^3\Delta$ by Azuma et al. [27], who also recorded the laser excitation spectra of the $C^3\Pi$–$X^3\Delta$, $e^1\Pi$–$X^3\Delta_2$ and $f^1\Phi$–$a^1\Delta$ transitions and measured the spin–orbit intervals by observation of weak satellite branches [28]. In this work the $X^3\Delta_2$–$X^3\Delta_1$ and $X^3\Delta_3$–$X^3\Delta_2$ intervals of 400.5 ± 0.1 and 490.5 ± 0.1 cm^{-1} were determined for the $X^3\Delta$ state of NbN. Azuma et al. [28] have also

* Corresponding author. Fax: +1 520 621 8407.
E-mail address: rram@u.arizona.edu (R.S. Ram).

0022-2852/$ - see front matter © 2007 Elsevier Inc. All rights reserved.
doi:10.1016/j.jms.2007.03.009

observed a number of transitions between the low-lying singlet and triplet electronic states by recording the wavelength resolved fluorescence following the selective laser excitation of different states and determined accurate term energy positions of the different spin components of the $A^3\Sigma^-$, $B^3\Pi$ and $C^3\Pi$ triplet states as well as the positions of the $a^1\Delta$, $b^1\Sigma^+$, $c^1\Gamma$, $e^1\Pi$ and $f^1\Phi$ singlet states of NbN [28].

There have been several theoretical calculations on NbN predicting the spectroscopic properties of the low-lying electronic states [29–32]. The most recent ab initio calculation by Langhoff and Bauschlicher [32] predicted the spectroscopic properties of the low-lying singlet and triplet electronic states of NbN. The ordering of states as well as the energy positions as determined experimentally by Azuma et al. [28] were found to be in excellent agreement with the predictions of Langhoff and Bauschlicher [32]. In a recent work on NbN [33] we recorded the emission spectrum of the red and near infrared regions of NbN using a Fourier transform spectrometer. Numerous electronic transitions have been observed between the low-lying singlet and triplet states. The analysis of new bands is consistent with the energy level diagram provided for NbN by Azuma et al. [28]. A missing $d^1\Sigma^+$ state, which was predicted by Langhoff and Bauschlicher [32] but not observed previously, was located by the observation of the $d^1\Sigma^+$–$A^3\Sigma_0^-$ and $d^1\Sigma^+$–$b^1\Sigma^+$ transitions [33].

In the present work, the emission spectrum of NbN has been reinvestigated in the 8000–35 000 cm^{-1} region using a Fourier transform spectrometer and some new transitions have been observed in the visible region. The bands observed in the 18 000–20 000 cm^{-1} region have been assigned as a new $^3\Pi$–$X^3\Delta$ transition while the bands observed in the 24 000–26 000 cm^{-1} region probably belong to a new $^3\Delta$–$X^3\Delta$ transition.

2. Experimental details

The details of the experimental set up and conditions used to observe the NbN bands have been provided in our previous papers on NbN [33] and NbCl [34]. In short, the molecules were produced in a microwave discharge lamp using a mixture of $NbCl_5$ vapor and about 3.0 Torr of He. NbN was observed as an impurity as no N_2 was added to the discharge mixture. The discharge tube was made of quartz and had an outside diameter of 12 mm. The emission from the lamp was sent directly into the entrance aperture of the 1-m Fourier transform spectrometer associated with the McMath–Pierce Solar Telescope of the National Solar Observatory at Kitt Peak. The spectra in the 8000–35 000 cm^{-1} region ware recorded in two parts. The 8000–20 000 cm^{-1} region was recorded using a UV beamsplitter, super blue Si diode detectors and an OG530 filter. The partial pressure of $NbCl_5$ vapor in the discharge tube was adjusted to maintained a bluish-white color. The NbN bands appeared strongly when the discharge was an intense blue–white color. A total of five scans co-added in about 35 min of integration at a resolution of 0.02 cm^{-1} was sufficient to obtain a spectrum with a signal-to-noise ratio suitable for rotational analysis. The 17 500–35 000 cm^{-1} region was recorded using the same setup except a $CuSO_4$ filter was used instead of the OG530 filter. This time the spectra were recorded at a resolution of 0.03 cm^{-1}.

The line positions were extracted from the observed spectra using a data reduction program called PC-DECOMP developed by J. Brault. The peak positions were determined by fitting a Voigt line shape function to each spectral feature. The branches in the different bands were sorted using a color Loomis–Wood program running on a PC computer. In addition to NbN, the spectra also contained some NbCl bands in the near infrared and several bands belonging to the doublet–doublet and quartet–quartet transitions of NbO throughout the entire region. Launila et al. [35] observed NbO bands using a similar source but used argon as the carrier gas. These authors used Ar atomic lines [36] for the calibration of their NbO spectra. In the absence of any suitable atomic or molecular lines needed for calibration, we used the NbO lines of some doublet–doublet transitions to transfer the calibration to the NbN spectra. The NbN lines in the 0–0 band appear with a maximum signal-to-noise ratio of about eight and the absolute accuracy of the wavenumber scale is expected to be of the order of ± 0.003 cm^{-1}. The accuracy of the measurements for the weaker and overlapped lines is limited to ± 0.007 cm^{-1}.

3. Description of observed bands

The new NbN bands are spread over the 18 000–26 000 cm^{-1} region. The carrier of these bands was established by rotational analysis of a number of strong bands. The spectrum at >18 000 cm^{-1} consists of two groups of bands, one in the 18 000–20 000 cm^{-1} region and the other in the 24 000–26 000 cm^{-1} region. The 18 000–20 000 cm^{-1} bands are stronger in intensity than the bands in the 24 000–26 000 cm^{-1} region. High-resolution spectra indicate that these two groups of bands involve $\Delta\Omega = -1$ and $\Delta\Omega = 0$ transitions, respectively.

3.1. The 18 000–20 000 cm^{-1} region ($^3\Pi$–$X^3\Delta$)

This region consists of three strong bands with R heads near 19 463.8, 19 659.0 and 19 757.0 cm^{-1}. A rotational analysis indicated that these bands involve $\Delta\Omega = -1$ transitions with the ground state of NbN as their lower state. These bands were assigned as 0–0 bands of the $^3\Pi_2$–$X^3\Delta_3$, $^3\Pi_1$–$X^3\Delta_2$ and $^3\Pi_{0\pm}$–$X\Delta_1$ subbands of a $^3\Pi$–$X^3\Delta$ transition. A compressed portion of the 0–0 band is presented in Fig. 1, where the R heads of the three subbands of the 0–0 band have been marked. The 0–1 bands of this transition were also identified easily in the 18 300–18 800 cm^{-1} region although they are much weaker than the 0–0 bands. The rotational structure in each subband consists of P, Q and R branches with the Q branch being the most intense.

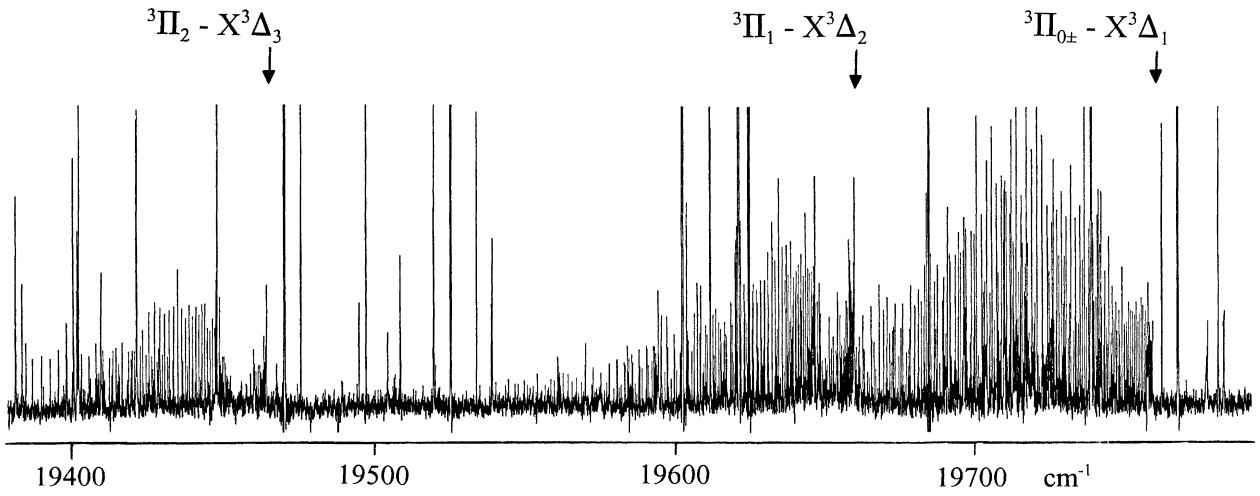

Fig. 1. A compressed portion of the spectrum showing the 0–0 bands of the three subbands of the $^3\Pi$–$X^3\Delta$ transition of NbN.

It was noted that the low J lines in the branches are relatively broad compared to the high J lines. This broadening is a result of nuclear hyperfine splitting since Nb nucleus has a large nuclear spin of 9/2 and a large nuclear magnetic moment of 6.1436 nuclear magnetons. Since the hyperfine structure was not resolved in our spectra due to limited resolution, the center of the peak of each broad rotational line was measured and used in the rotational analysis. The J assignment in the different bands was made by comparing the combination differences for common vibrational levels.

Our analysis indicates that the excited $^3\Pi_{0\pm}$, and $^3\Pi_1$ spin components are affected strongly by interactions with some nearby state (or states). The $^3\Pi_{0+}$ and $^3\Pi_{0-}$ components of the $^3\Pi_0$ spin component are separated by about 3.9 cm^{-1}. An attempt to fit the two levels together was unsuccessful since the interaction affects the two levels differently; the two levels were therefore treated as different states in the final fit. In addition to the usual constants T_v, B_v and D_v, higher order constants H_v and L_v are also required in the fit. The presence of interaction is also apparent from the negative values of the D_v and H_v constants.

Our rotational analysis indicates that the $^3\Pi_1$ spin component is also affected by similar perturbations. An attempt to fit the $^3\Pi_{1e}$ and $^3\Pi_{1f}$ components together does not provide a satisfactory fit and, in the end the e and f components were treated as different states. These levels also require higher order constants which have abnormal magnitudes. The e and f labels for the two parities were chosen arbitrarily. A local perturbation was observed near $J' = 22$ of the e-parity and a number of lines from $J' = 11$–32 were given reduced weights. For the f-parity levels the lines with $J' < 18$ and $J' > 32$ are affected by perturbations and were de-weighted.

The $^3\Pi_2$ level is relatively free from perturbations, except for lines with high J values. The e- and f-parity levels of this substate are not resolved because of negligible Ω doubling. An expanded portion of the 19463.8 cm^{-1} band is provided in Fig. 2. This subband is free from any local perturbation for lower J values while the high J lines after

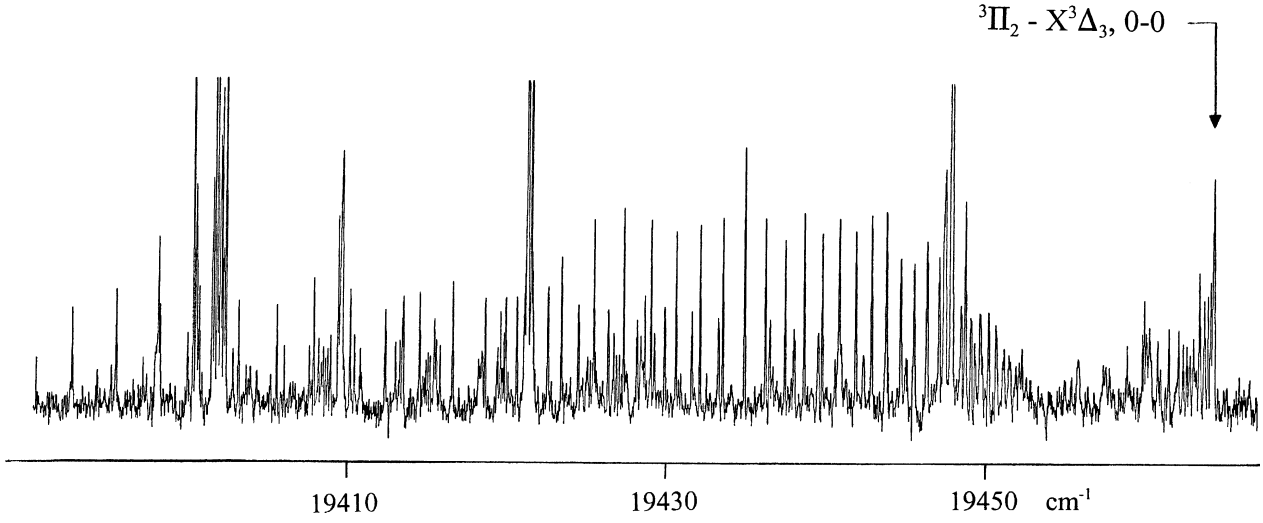

Fig. 2. An expanded portion of the 0–0 band of the $^3\Pi_2$– $X^3\Delta_3$ subband of NbN.

$J' = 33$ are affected by interactions and the intensity suddenly drops after $J' = 36$.

3.2. The 24000–26000 cm^{-1} region ($^3\Delta$–$X^3\Delta$?)

To higher wavenumbers, a group of very weak bands were observed which involve $\Delta\Omega = 0$ transitions. The 0–0 bands have R heads located near 25409.9, 25518.7 and 25534.7 cm^{-1}. A rotational analysis of these bands indicates that the two bands with R heads at 25518.7 and 25534.7 cm^{-1} have the $X^3\Delta_1$ ground state spin component as the lower state while the band with the R head at 25409.9 cm^{-1} has the $X^3\Delta_2$ spin component as its lower state. We were unable to identify any band having the $X^3\Delta_3$ spin component as its lower state. Two of the observed bands perhaps belong to a new $^3\Delta$–$X^3\Delta$ transition of NbN. A compressed portion of the 0–0 bands near the R heads is provided in Fig. 3, where the R heads have been marked with vertical arrows. For the 25518.7 and 25534.7 cm^{-1} bands we have identified the rotational lines up to $R(36)$, $P(33)$ and $R(21)$, $P(22)$, respectively. No higher vibrational bands were observed for the two subbands. The $^3\Delta_2$–$X\ ^3\Delta_2$ subband is the strongest of the three and we were able to identify the 0–1, 0–0 and 1–1 bands. An expanded portion of the 0–0 band is provided in Fig. 4, in which some low J, R and P branch lines have been marked. Rotational lines up to $R(47)$ and $P(51)$ have been identified in the 0–0 band. The lower J lines ($<J' = 16$) of the $v = 0$ level of the excited state are affected by perturbations. Also a local perturbation has been observed at $J' = 27$ shifting $R(26)$ and $P(28)$ lines by about -0.25 cm^{-1}. This perturbation can clearly be seen in the R lines of Fig. 4. Higher order spectroscopic parameters H_v and L_v are also required in order to minimize the standard deviation of the fit. This as well as the negative values of the constants D_v and H_v are a reflection of interactions in the excited state. The $v' = 1$ vibrational level of the excited state has also been identified from the observation of the 1–1 band. The $v' = 1$ vibrational level is relatively less affected by perturbations.

4. Results and discussion

In their laser excitation work on NbN, Merer (private communication) observed two isolated bands with R heads at 18431 and 18284 cm^{-1} which they tentatively assigned as the 1–1 and 5–4 bands of the $^3\Pi_2$–$X^3\Delta_3$ transition which they called the Y–X transition. No other bands belonging to this transition were observed although they located many other isolated bands in the same region, which were referred to as charge transfer bands. The observation of the 0–0 bands of the new $^3\Pi$–$X^3\Delta$ transition in the 18000–20000 cm^{-1} region has enabled us to reassign the 18431 cm^{-1} band as the 0–1 band of the $^3\Pi_2$–$X^3\Delta_3$ subband of the new transition. The 18284 cm^{-1} band observed by Merer (private communication) has not been observed in our spectra. The rotational lines of the 18431 cm^{-1} band reported by Merer (private communication) agree very well with our measurements although this band is much weaker in our spectra. We have fitted their measurements of this band with our data in the final fit.

Although the first lines were not identified in any bands in our spectra because of overlapping by returning R lines after formation of the head, there is no doubt in the assignment since these bands are interconnected by common vibrational levels. Moreover, the observed lower state combination differences agree well with the values obtained from the previous studies of NbN [33,34]. The molecular constants were determined by fitting the observed line positions to the following customary energy level expression:

$$F_v(J) = T_v + B_vJ(J+1) - D_v[J(J+1)]^2 + H_v[J(J+1)]^3 + L_v[J(J+1)]^4$$

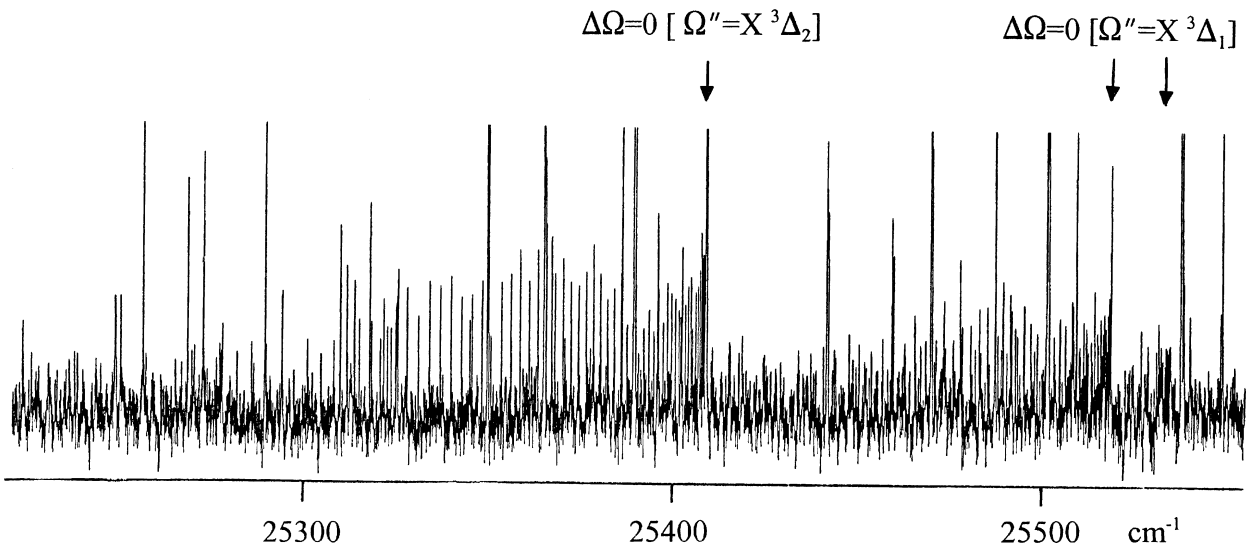

Fig. 3. A compressed portion of the spectrum of the $\Delta\Omega = 0$ bands of NbN with the R heads of observed subbands marked.

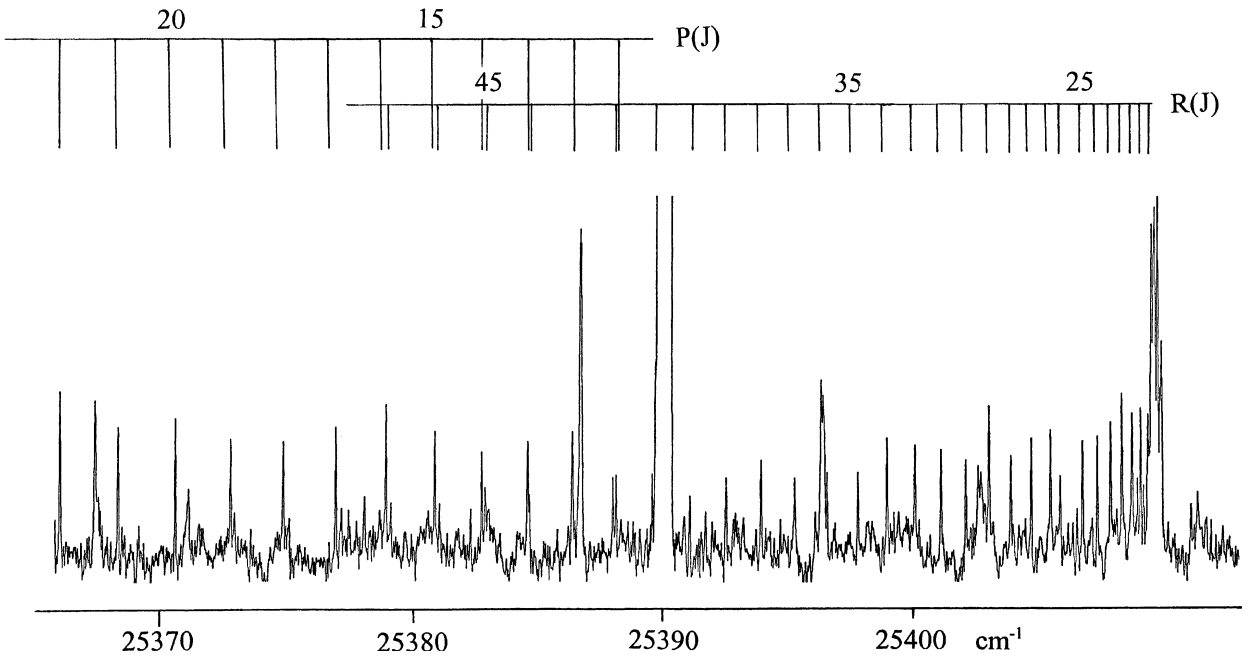

Fig. 4. An expanded portion of the 0–0 band of the $\Delta\Omega = 0$, $\Omega'' = 2$ transition with some low J rotational lines marked.

In the final fit the badly blended lines were given reduced weights and overlapped lines were excluded in order to improve the standard deviation. The bands of the two new transitions were initially fitted separately. In the final fit, however, the lines of the different subbands of both transitions that have vibrational levels in common were combined and a fit was obtained to determine a single set of molecular constants for each vibrational level of the different spin components. The spectroscopic constants obtained in the final fit are provided in Table 1 (Also, see Supplementary data).

The ground state of NbN is very well characterized from the previous spectroscopic studies. The present constants for the ground state agree very well with the values reported previously. Since we observed only the $v = 0$ vibrational levels of the $^3\Pi_{0\pm}$, $^3\Pi_1$ and $^3\Pi_2$ spin components, no vibrational intervals or equilibrium spectroscopic constants were determined for the excited state. The same is true for the two $\Delta\Omega = 0$, $\Omega'' = 1$ bands with R heads at 25 518.7 and 25 534.7 cm^{-1}. For the $\Delta\Omega = 0$, $\Omega'' = 2$ transition we have observed the 0–0, 0–1 and 1–1 bands. The analysis of these bands places the $v = 0$ and 1 vibrational

Table 1
Molecular constants (in cm^{-1}) for the observed states of NbN

State	v	T_v	B_v	$10^5 \times D_v$	$10^8 \times H_v$	$10^{12} \times L_v$
$\Omega = 2$	1	26705.3901(86)	0.467263(45)	0.1060(51)	—	—
	0	25802.7414(79)	0.470401(33)	−0.0802(41)	−0.0480(21)	0.0553(39)
$\Omega = 1$	0	25526.715(15)	0.469960(40)	0.0543(23)	—	—
$\Omega = 1$	0	25511.9662(55)	0.466274(59)	0.196(11)	—	—
$^3\Pi_2$	0	20343.8311(63)	0.481040(46)	0.179(13)	0.169(17)	−1.364(73)
$^3\Pi_{1f}$	0	20048.3546(66)	0.479566(27)	−0.0770(28)	−0.0369(11)	0.0335(14)
$^3\Pi_{1e}$	0	20046.6898(36)	0.483164(31)	0.2493(43)	0.0754(23)	−0.1070(39)
$^3\Pi_{0-}$	0	19752.1990(34)	0.449881(29)	−2.3552(66)	−1.0180(65)	1.460(22)
$^3\Pi_{0+}$	0	19748.321(22)	0.41604(12)	−6.794(23)	−3.567(19)	7.155(54)
$^3\Delta_3$	1	1924.9640(48)	0.499900(25)	0.0441(17)	—	—
	0	891.0[a]	0.502531(24)	0.0466(15)		
$^3\Delta_2$	1	1434.5614(27)	0.499154(11)	0.04742(36)	—	—
	0	400.5[a]	0.501742(10)	0.04722(32)		
$^3\Delta_1$	1	1033.7493(21)	0.497572(17)	0.04675(87)	—	—
	0	0.0[a]	0.500161(16)	0.04777(86)		

[a] Fixed values.

levels at 25802.75 and 26705.41 cm^{-1} above the ground state. This provides the vibrational interval of $\Delta G_{1/2} = 902.6604(98)\ cm^{-1}$ for the excited $\Omega = 2$ state. The equilibrium rotational constants for this state using the constants of Table 1 are $B_e = 0.472028(44)\ cm^{-1}$ and $\alpha_e = 0.003182(56)\ cm^{-1}$.

NbN has a $^3\Delta_r$ ground state which arises primarily from the electron configuration $5s\sigma^1 4d\delta^1$. This configuration also results in a low-lying $^1\Delta$ state. The other low-lying excited electronic states arise from the promotion of the $5s\sigma$ or $4d\delta$ electrons to higher Nb-centered molecular orbitals as given below:

$$5s\sigma^2 \qquad {}^1\Sigma^+ \tag{1}$$

$$4d\delta^2 \qquad {}^1\Sigma^+\ {}^3\Sigma^-\ {}^1\Gamma \tag{2}$$

$$4d\delta^1 4d\pi^1 \qquad {}^3\Phi_r,\ {}^3\Pi_r\ {}^1\Pi\ {}^1\Phi \tag{3}$$

$$5s\sigma^1 4d\pi^1 \qquad {}^3\Pi_r\ {}^1\Pi \tag{4}$$

$$4d\delta^1 4d\sigma^1 \qquad {}^3\Delta_r\ {}^1\Delta \tag{5}$$

All of the states arising from the ground state configuration as well as low-lying configurations (1)–(3) have been observed experimentally by Azuma et al. [28] and Ram and Bernath [33]. The new $\Delta\Omega = -1$ transition observed in the 18000–20000 cm^{-1} region is probably the $5s\sigma^1 4d\pi^1\ {}^3\Pi$–$5s\sigma^1 4d\delta^1\ X^3\Delta$ electronic transition. The other $\Delta\Omega = 0$ bands located in the 24000–26000 cm^{-1} region probably belong to the $4d\delta^1 4d\sigma^1\ {}^3\Delta$–$5s\sigma^1 4d\delta^1\ X^3\Delta$ transition.

Langhoff and Bauschlicher [32] have used state averaged complete-active-space self-consistent-field (CASSCF) multi reference configuration-interaction (MRCI) calculations to predict almost all of the singlet and triplet states below about 20000 cm^{-1}: namely, $X^3\Delta$, $A^3\Sigma^-$, $B^3\Phi$, $C^3\Pi$, $a^1\Delta$, $b^1\Sigma^+$, $c^1\Gamma$, $d^1\Sigma^+$ $e^1\Pi$. They also calculated the ordering of the states in the singlet manifold. All of these states were observed except the $d^1\Sigma^+$ state, which has also been recently identified near 13908 cm^{-1} relative to the lowest $X^3\Delta_1$ spin component of the ground state [34]. Other higher-lying states in the singlet and triplet manifolds states, for example the $f^1\Phi$ state and the new $^3\Pi$ ($5s\sigma^1 4d\pi^1$) and $^3\Delta$ ($4d\delta^1 4d\sigma^1$) states were not included in the calculations of Langhoff and Bauschlicher [32].

5. Conclusions

The emission spectrum of NbN has been investigated in the 8000–35000 cm^{-1} region using a Fourier transform spectrometer. New bands observed in the 18000–26000 cm^{-1} region have been assigned to two new electronic transitions. Several bands located in the 18000–20000 cm^{-1} region have been identified as the 0–1 and 0–0 bands of the $^3\Pi_{0\pm}$–$X\Delta_1$, $^3\Pi_1$– $X^3\Delta_2$ and $^3\Pi_2$–$X^3\Delta_3$ subbands of a $^3\Pi$–$X^3\Delta$ transition. Another group of very weak bands observed in the 24000–26000 cm^{-1} region has been assigned to a $\Delta\Omega = 0$ transition which probably belong to a $^3\Delta$–$X^3\Delta$ transition. A rotational analysis of a number of bands has been obtained and molecular constants have been determined for the new states. The present observations indicate that both excited states interact with some close lying states causing global and local perturbations. No theoretical predictions are available for the new excited states of NbN.

Acknowledgments

We thank Prof. A. J. Merer for providing us a copy of the Ph.D. thesis of G. Huang which contains some unpublished data on NbN. We also thank M. Dulick of the National Solar Observatory for assistance in obtaining the spectra. The National Solar Observatory is operated by the Association of Universities for Research in Astronomy, Inc., under contract with the National Science Foundation. The research described here was supported by funding from the NASA laboratory astrophysics program. Support was also provided by the Natural Sciences and Engineering Research Council of Canada.

Appendix A. Supplementary data

Supplementary data associated with this article are available on ScienceDirect (www.sciencedirect.com) and as part of the Ohio State University Molecular Spectroscopy Archives (http://msa.lib.ohio-state.edu/jmsa_hp.htm).

References

[1] D.N. Davis, Astrophys. J. 106 (1949) 28–75.
[2] H. Spinard, R.F. Wing, Annu. Rev. Astron. Astrophys. 7 (1969) 269–302.
[3] C. Jascheck, M. Jascheck, The Behavior of Chemical Elements in Stars, Cambridge University Press, Cambridge, 1995.
[4] R.S. Ram, P.F. Bernath, J. Chem. Phys. 96 (1992) 6344–6347.
[5] R.S. Ram, P.F. Bernath, J. Mol. Spectrosc. 165 (1994) 97–106.
[6] R.S. Ram, P.F. Bernath, J. Mol. Spectrosc. 184 (1997) 401–412.
[7] R.S. Ram, P.F. Bernath, J. Opt. Soc. Am. 11B (1994) 225–230.
[8] R.S. Ram, P.F. Bernath, W.J. Balfour, J. Cao, C.X.W. Qian, S.J. Rixon, J. Mol. Spectrosc. 168 (1994) 350–362.
[9] W.J. Balfour, J. Cao, C.X.W. Qian, S.J. Rixon, J. Mol. Spectrosc. 183 (1997) 113–118.
[10] W.J. Balfour, C.X.W. Qian, C. Zhou, J. Chem. Phys. 106 (1997) 4383–4388, 107 (1997) 4473–4482.
[11] S.G. Fougère, W.J. Balfour, J. Cao, C.X.W. Qian, J. Mol. Spectrosc. 199 (2000) 18–25.
[12] E.J. Friedman-Hill, R.W. Field, J. Chem. Phys. 100 (1994) 6141–6152.
[13] K.Y. Jung, T.C. Steimle, D. Dai, K. Balasubramanian, J. Chem. Phys. 102 (1995) 643–652.
[14] A.J. Marr, M.E. Flores, T.C. Steimle, J. Chem. Phys. 104 (1996) 8183–8196.
[15] R.S. Ram, J. Liévin, P.F. Bernath, J. Chem. Phys. 109 (1998) 6329–6337.
[16] K.L. Kunze, J.F. Harrison, J. Am. Chem. Soc. 112 (1990) 3812–3825.
[17] I. Shim, K.A. Gingerich, Int. J. Quant. Chem. 46 (1993) 145–157.
[18] C.W. Bauschlicher Jr., Chem. Phys. Lett. 100 (1983) 515–518.
[19] S.M. Mattar, J. Phys. Chem. 97 (1993) 3171–3175.
[20] J.F. Harrison, J. Phys. Chem. 100 (1996) 3513–3519.
[21] S.M. Mattar, B.J. Doleman, Chem. Phys. Lett. 216 (1993) 369–374.
[22] P.E.M. Siegbahn, M.R.A. Blomberg, Chem. Phys. 87 (1984) 189–201.
[23] M.R.A. Blomberg, P.E.M. Siegbahn, Theor. Chim. Acta 81 (1992) 365–374.

[24] A. Fiedler, S. Iwata, Chem. Phys. Lett. 271 (1997) 143–151.
[25] T.M. Dunn, K.M. Rao, Nature 222 (1969) 266.
[26] J.-L. Féménias, C. Athénour, T.M. Dunn, J. Chem. Phys. 63 (1975) 2861–2868.
[27] Y. Azuma, A. Barry, M.P.J. Lyne, A.J. Merer, J.O. Schröder, J.-L. Féménias, J. Chem. Phys. 91 (1989) 1–12.
[28] Y. Azuma, A. Barry, G. Huang, M.P.J. Lyne, A.J. Merer, V.I. Srdanov, J. Chem. Phys. 100 (1994) 4138–4155.
[29] A. Bées, S.A. Mitchell, M.Z. Zgierski, J. Phys. Chem. 102 (1998) 6340–6347.
[30] H. Sellers, J. Phys. Chem. 94 (1990) 1338–1343.
[31] D.A. Fletcher, D. Dai, T.C. Steimle, K. Balasubramanian, J. Chem. Phys. 99 (1993) 9324–9325.
[32] S.R. Langhoff, C.W. Bauschlicher Jr., J. Mol. Spectrosc. 143 (1990) 169–179.
[33] R.S. Ram, P.F. Bernath, J. Mol. Spectrosc. 201 (2000) 267–279.
[34] R.S. Ram, N. Rinskopf, J. Liévin, P.F. Bernath, J. Mol. Spectrosc. 228 (2004) 544–553.
[35] O. Launila, J. Mol. Spectrosc. 229 (2005) 31–38.
[36] G. Norlen, Phys. Scr. 8 (1973) 249–268.